Journal of Climate

Atmospheric Response to the Weddell Sea Polynya

--Manuscript Draft--

Manuscript Number:	JCLI-D-16-0120
Full Title:	Atmospheric Response to the Weddell Sea Polynya
Article Type:	Article
Abstract:	The occurrence of the Weddell Polynya has been explained in numerous studies. Its atmospheric response, however, has been treated in fewer investigations, mostly based on coarse resolution data and/or model output. Here we advance our understanding of the atmospheric response to the Weddell polynya by analyzing the results from an atmospheric and oceanic synoptic-scale resolving Community Earth System Model (CESM) simulation. While coarser-resolution versions of CESM generally do not produce open-ocean polynyas in the Weddell Sea, they do emerge and disappear on interannual timescales in the synoptic-scale simulation. This provides an ideal opportunity to study the polynya's impact on the overlying and surrounding atmosphere. Our results indicate significant local impacts on turbulent heat fluxes, precipitation, cloud characteristics, and the shortwave radiative balance. Impacts are found to be sensitive to the synoptic wind direction. Strongest regional impacts are found when northeasterly winds cross the polynya and interact with katabatic winds. Large-scale impacts of the polynya manifest themselves in surface air pressure anomalies, but are only found to be significant when cold, dry air masses strike over the polynya, i.e. in case of southerly winds.

Atmospheric Response to the Weddell Sea Polynya

Wilbert Weijer*, Milena Veneziani,

Los Alamos National Laboratory, Los Alamos, New Mexico, United States

Achim Stössel

Texas A&M University, College Station, TX, United States

Matthew W. Hecht, Nicole Jeffery, Alexandra Jonko

Los Alamos National Laboratory, Los Alamos, New Mexico, United States

and Travis Hodos

United States Air Force Academy, Colorado Springs, Colorado, United States

**Corresponding author address:* Wilbert Weijer, Los Alamos National Laboratory, MS B214, Los Alamos, NM 87545.

E-mail: wilbert@lanl.gov

ABSTRACT

The occurrence of the Weddell Polynya has been explained in numerous studies. Its atmospheric response, however, has been treated in fewer investigations, mostly based on coarse resolution data and/or model output. Here we advance our understanding of the atmospheric response to the Weddell polynya by analyzing the results from an atmospheric and oceanic synoptic-scale resolving Community Earth System Model (CESM) simulation. While coarser-resolution versions of CESM generally do not produce open-ocean polynyas in the Weddell Sea, they do emerge and disappear on interannual timescales in the synoptic-scale simulation. This provides an ideal opportunity to study the polynya's impact on the overlying and surrounding atmosphere. Our results indicate significant local impacts on turbulent heat fluxes, precipitation, cloud characteristics, and the shortwave radiative balance. Impacts are found to be sensitive to the synoptic wind direction. Strongest regional impacts are found when northeasterly winds cross the polynya and interact with katabatic winds. Large-scale impacts of the polynya manifest themselves in surface air pressure anomalies, but are only found to be significant when cold, dry air masses strike over the polynya, i.e. in case of southerly winds.

1. Introduction

Polynyas are areas of open water within the winter ice pack. They facilitate a strong heat exchange between the atmosphere and ocean, and often feature intense sea ice production. Antarctic polynyas are thought to play a key role in the formation of Antarctic Bottom Water (AABW; Zwally et al. 1985), the most voluminous water mass in the World's Ocean (Johnson 2008). Polynyas also often sustain high levels of biological productivity (e.g., Smith Jr. and Gordon 1997).

Mechanically-forced (coastal) polynyas are a ubiquitous feature of the Antarctic coastal environment, as in many places cold katabatic winds push newly formed sea ice away from the land, keeping the coastal waters virtually ice free (e.g., Adolphs and Wendler 1995). Convectively-forced, or open-ocean polynyas, however, are more enigmatic, as they require an ocean heat source to keep the polynya ice free. The most spectacular example is the Weddell Polynya, a large sustained polynya that was observed in the mid-70s, but has not appeared since (Zwally and Gloersen 1977; Carsey 1980). This polynya was associated with deep convection that tapped into the heat of the relatively warm Circumpolar Deep Water (Martinson et al. 1981; Gordon 1982); it may have been preconditioned by an anomalously strong Weddell Gyre (Gordon et al. 2007; Cheon et al. 2015) and triggered by ocean-topography interaction at Maud Rise (Holland 2001). de Lavergne et al. (2014) argue that the Weddell Polynya was most likely a frequently appearing feature up until the one time it was observed in the mid-70s, in the early days of remote sensing. If so, then the absence of the Weddell Polynya since that time would have to be understood as representing a significant regime shift that would be convolved with other changes involving deep waters today.

Smaller open-ocean polynyas, like the Cosmonaut polynya (Comiso and Gordon 1987), are more transient of nature and may rely more on divergent sea ice transport induced by atmospheric forcing (Arbetter et al. 2004; Bailey et al. 2004), along with the upwelling of warm waters due to Ekman suction (Prasad et al. 2005) or ocean dynamics (Comiso and Gordon 1996). Reviews of polynya studies can be found in Smith et al. (1990); Maqueda et al. (2004); Williams et al. (2007).

Understanding the conditions under which polynyas form, and the effect that they have on the state of the ocean and atmosphere, is important. In fact, the current generation of climate models varies widely in its representation of polynyas and the convective state of the Weddell Sea in particular (Heuzé et al. 2013; de Lavergne et al. 2014; Downes et al. 2015; Stössel et al. 2015). Even different configurations of the same model code (for instance with eddying and non-eddying resolutions) can exhibit contrasting behavior, as is the case with the model used for this study. The impact of open-ocean polynyas on the stratification of the Southern Ocean and the characteristics of Antarctic Bottom Water has been the subject of several studies (e.g. Stössel et al. 2002; Heuzé et al. 2013; Downes et al. 2015). The extent to which the presence or absence of polynyas can account for differences in the mean state of the atmosphere has remained an open question.

Assessing the influence that large and persistent open-ocean polynyas have on the atmosphere has been hindered by the difficulty of observing the atmospheric state in the Antarctic ice zone, especially during winter months; as well as by the absence of the Weddell Polynya for the past 4 decades. Working within these limitations, Moore et al. (2002) reconstruct the atmospheric influence of the 1976 Weddell Polynya using a reanalysis of the atmospheric state during the period of its presence. They report 20°C warmer air temperatures, 20% more cloud cover (up to 70% total coverage), 6-8 hPa lower sea level pressure over the Weddell Polynya compared to climatology, and sensible and latent heat flux anomalies on the order of 150 W m^{-2} and 50 W m^{-2}, respectively. Although their analysis shows enhanced precipitation by 0.5-1 mm day^{-1}, they argue that evaporation exceeds precipitation, resulting in net freshwater *loss* from the ocean due to the polynya.

The atmospheric response to polynyas has also been the subject of several modeling studies. Dare and Atkinson (1999, 2000) show how turbulent heat fluxes increase the buoyancy over the polynya, generating a turbulent plume that mixes high-momentum air downward. The resulting acceleration of the flow over the polynya leads to divergence and downdrafts on the upwind side of the polynya, and convergence and updrafts on the downwind side. The increased flow speed is aided by reduced surface drag over the open water compared to the surrounding ice pack. Timmermann et al. (1999) argue that the thermal perturbation over polynyas can cause a low pressure anomaly, but note that the mean cross-polynya flow needs to be sufficiently weak (< 1 m s^{-1}) for the thermal anomaly to affect the lower atmosphere.

Glowienka-Hense (1995) performed a dedicated sensitivity experiment using a coarse-resolution atmospheric general circulation model to study the global atmospheric response to the Weddell Polynya. She compared simulations with and without the Weddell Polynya under perpetual July conditions, and found impacts throughout the entire southern hemisphere. Most notable responses included a warming of the lower atmosphere, but a cooling of the upper troposphere; a deepening of the circumpolar trough between 40° and 60°S, and an overall intensification of the mean circulation globally.

Minnett and Key (2007) review existing literature about meteorology and atmosphere/surface coupling in polynyas, with a focus on the Arctic. They find a shift in cloud distribution towards multiple cloud types at several atmospheric levels and an elevated occurrence of cumuliform cloud types, compared with observations over sea and landfast ice.

Here we attempt to refine estimates of the impact of the Weddell Polynya on the atmosphere that may occur either through changes in the regional circulation or the heat flux balance. The continuing development of coupled climate models towards resolving increasingly smaller scales is now producing coupled climate simulations of centennial length. Here we will take advantage of a new state-of-the-art high-resolution climate simulation (Small et al. 2014) that allows us to study the atmospheric response to polynyas in unprecedented detail. Our focus here is on the impact of the Weddell Polynya on the atmosphere aloft; in a follow-up paper we will analyze the role of the ocean in the generation and maintenance of the polynya in these and similar simulations.

2. Methods

To study the atmospheric response to the Weddell Sea Polynya, we use output from the high-resolution coupled climate system simulation described by Small et al. (2014). The well-documented Community Earth System Model version 1 (CESM1) they employed is widely used for investigations of climate variability and change (Hurrell et al. 2013). This simulation was run during the Accelerated Scientific Discovery (ASD) phase of the platform Yellowstone, and is among the first efforts to run CESM in a high-resolution configuration that explicitly resolves mesoscale features in the ocean. The ocean component is the Parallel Ocean Program version 2 (POP2) configured at a nominal resolution of 0.1°. It is coupled to a sea ice simulator at the same resolution, the Los Alamos Sea Ice Model version 4 (CICE4). The atmosphere component is the Community Atmosphere Model version 5 (CAM5) configured at an approximate 0.25° resolution of the Spectral Element (SE) dynamical core. The model was run for 100 years under fixed radiative forcing conditions representative of year 1990. Output from this simulation is available for download through the Earth System Grid. Model fields are mostly saved as monthly averaged fields, but a limited number of variables are available as daily averages. A companion run at nominal (and standard) 1° ocean and atmosphere resolutions was also performed. We analyzed this lower resolution simulation and could not identify polynyas in the Weddell Sea in any year.

In the first decades of the high-resolution simulation, the ice pack in the Southern Ocean is quite unrealistic, with large areas of open water in the Weddell Sea in winter. In subsequent years the sea ice cover becomes more realistic, albeit remaining highly variable. Polynyas, either fully enclosed or large embayments connected to the greater (ice-free) Southern Ocean, are featured in most years; years with a full ice cover are rare.

A polynya is defined here as an enclosed region within the Antarctic ice pack that has ice fractions below 15%. We focus on the 3 winter/spring months of August, September and October (ASO). For this study we selected three years (68, 76 and 80) that feature a polynya that is fully enclosed for the entire 3 month period (Fig. 1). The polynyas in these 3 years appear at approximately the same location and are comparable in size ($1.1, 0.8$ and $1.4 \times 10^5\,\mathrm{km}^3$, respectively). This is a factor of 2 to 3 smaller than the polynya observed in the Weddell Sea between 1974 and 1976 ($2-3 \times 10^5\,\mathrm{km}^3$; Carsey 1980). For calculating polynya-averaged quantities, we define polynya masks based on the 15% contour of the ASO-averaged sea ice fraction for each year.

To distinguish the impact of the polynyas on the overlying and surrounding atmosphere, we contrast the associated atmospheric conditions with those emerging in non-polynya years. To that end, we also selected three years with full sea ice cover (63, 64 and 72). We defined a "polynya mask" for these non-polynya years by averaging the ASO sea ice fractions of the 3 polynya years, and taking the 45% contour to make sure that the mask encompasses the region covered by the three individual polynyas (red contour in Fig. 1).

We show the annual time series of polynya-averaged quantities, as well as vertical profiles of polynya-averaged quantities for the ASO trimester. Given the low number of degrees of freedom associated with just a few years' worth of monthly averaged quantities, no attempt was made to formally test the significance of the differences in the mean. We cautiously indicate as "significant" a difference in the mean that is outside the envelope of the individual years.

The directional analyses are based on the daily direction of the winds over the polynya. This direction is calculated from the polynya-averaged components of the surface velocity. We divide the daily-averaged fields into 5 directional categories: The category referred to as ‘Central’ (CE) consists of days for which the polynya-averaged winds are less than 5 m s^{-1}, regardless of direction. The northeasterly (NE), northwesterly (NW), southwesterly (SW) and southeasterly (SE) categories refer to days during which polynya-averaged winds exceed 5 m s^{-1} and come from the indicated direction. Differences between means are tested using the Student’s *t*-test, following von Storch and Zwiers (1999, p.112).

3. Results

Seasonal evolution, polynya vs. non-polynya years

Figure 2 shows the annual evolution of several atmospheric variables, for polynya (red) and non-polynya (blue) years. For non-polynya years, ice fraction passes through the 15% level in June, and reaches 90% in September; by construction, polynya-averaged sea ice fractions remain below 15% for polynya years. The polynyas are very stable in their extent and shape, and remain consistently ice-free throughout the winter season. This suggests that the cause of the polynya is oceanic in nature, and that synoptic atmospheric variability is not responsible for maintaining the polynya. This is in contrast to the role often ascribed to synoptic atmospheric variability in the generation and maintenance of the highly variable Cosmonaut Polynya (Arbetter et al. 2004; Bailey et al. 2004; Prasad et al. 2005). Consequently, we may focus on the impact, rather than response, of a sensible heat polynya on the atmosphere.

Surface temperatures (TS) differ strongly between polynya and non-polynya years; TS in polynya years is limited by the freezing temperature of sea water ($\approx$ 271 K), while the surface of the sea ice in non-polynya years dips down to 257 K. Near-surface air temperatures (TBOT) drop to only 265 K for polynya years whereas they get as low as 257 K for non-polynya years; TS and TBOT are hence almost equalized for non-polynya years, while a significant ($\mathcal{O}(6K)$) temperature contrast persists over polynyas. The higher atmospheric surface temperatures are also reflected in the humidity (QBOT), which is significantly higher for the August-November period during polynya years.

Wind speeds at the 10 m level (U10) are significantly reduced for ice-covered conditions. This is at least partly a result of enhanced surface friction over sea ice compared to the ice-free ocean (Andreas et al. 1984). The rapid decline in U10 from its maximum in June through its minimum in September corresponds to the increase in sea ice concentration.

The absence of sea ice cover in polynya years has a clear impact on the balance of sensible (SHLFX) and latent (LHFLX) heat fluxes. After a gradual increase in the first 5 months, these turbulent fluxes sharply decrease after mid-June during non-polynya years. This is partly due to a reduced temperature contrast and reduced wind speed. SHFLX hovers around 10 W m^{-2} from August onward, while LHFLX bottoms out below 10 W m^{-2} in early September. For polynya years, SHFLX peaks in August at 135 W m^{-2} and LHFLX at 89 W m^{-2}. So sensible and latent heat fluxes are typically 100 W m^{-2} and 70 W m^{-2} higher over polynyas compared to non-polynya years. Integrated over the polynya area and over the year, the excess heat transfer is 114 EJ (1 EJ = 10^{18} J) and 87 EJ respectively.

There is a pronounced impact of the presence of polynyas on the net shortwave radiation at the top of the atmosphere (FSNT), which is equal to the impact at the surface (not shown). The absence of sea ice in polynyas strongly reduces the albedo and increases absorption of shortwave solar radiation. Although this difference only manifests itself in the months where the sun actually has a significant input (from August onward), the net heat uptake by the ocean increases by 67 EJ in polynya years.

Surprisingly, there is hardly a discernible impact of polynyas on the net longwave radiative budget at the surface (FLNS). FLNS is only slightly higher (6 EJ) during polynya years than during non-polynya years; a difference that is reduced to 3 EJ at the top of the atmosphere (not shown). We found that the enhanced emission of longwave radiation from polynyas due to the higher surface temperature is almost fully compensated by increased *downward* fluxes. This is most likely due to changes in cloud cover or properties. However, there is no evidence for this in the total cloud fraction (CLDTOT), which is extremely high over the Antarctic ice pack in both polynya and non-polynya years, with averages exceeding 97% in August. Instead, we do find support for the hypothesis that polynyas have a significant influence on clouds aloft in the vertical structure of the atmospheric column, which we explore in the next section.

Polynya years experience more precipitation (PRECT; roughly by 1 mm/day) from July through November. However, polynyas do not seem to have an impact on the surface pressure distribution (PSL), nor the pressure field aloft (not shown). We will return to this issue in our directional analysis based on daily averaged fields.

Vertical structure

Analysis of the vertical structure of the atmosphere over polynyas reveals a distinct difference in cloud structure (Fig. 3). Cloud fraction (CLOUD) between 200 and 800 hPa hovers around 30% for non-polynya years and is about 5% higher in polynya years. However, the largest difference is found below 800 hPa. Non-polynya years have a maximum in cloud fraction (60%) just above the surface (ice fog), while the maximum (68%) in polynya years is elevated to 900 hPa. This shift is echoed in relative humidity (RELHUM), and enhanced specific humidity (Q) below 800 hPa. These high cloud fractions explain the column total cloud fraction (CLDTOT) in Fig. 2.

In addition to the upward shift in cloud amount during polynya years, we observe a distinct difference in the cloud composition. The clouds in polynya years contain large amounts of water (ICLDLWP) and ice (ICLDIWP), relative to the dry cloud deck in non-polynya years. The cloud level in polynya years is associated with a maximum in updraft at 900 hPa, represented here by its associated heat transport (-OMEGAT), which is absent in non-polynya years. In addition, turbulent fluxes, reflected by turbulent kinetic energy (TKE), are considerably enhanced in polynya years below 750 hPa. These factors suggest that the turbulent convection and updrafts generated by polynyas generate clouds of convective nature. We deduce that the high water and ice content of these clouds are responsible for the enhanced downward longwave radiation that balances the enhanced emissions of the warmer surface of polynyas.

Although there is a large interannual spread in vertical velocities, they are on average higher in polynya years throughout the atmospheric column. This difference may be responsible for the slightly (5%) enhanced cloud fractions above 800 hPa.

Directional analysis

Figure 2 shows that, on monthly time scales, there is no discernible difference in sea level pressure between polynya and non-polynya years. In this section we analyze how the atmospheric response to polynyas depends on the wind direction on a daily time scale. To that end we categorize the available daily averaged fields according to prevailing wind direction, average over those directional subsets, and determine differences between polynya and non-polynya years (Fig. 4). Table 1 shows the number of days for each category for all polynya and non-polynya years, showing close tallies. The most prevalent wind conditions are southwesterly (SW) and quiet conditions (CE). Note that only a few variables were saved on a daily basis, so this analysis is limited by the available data. Also, to focus on the regional response of SLP, we average daily SLP over our analysis region and remove this average from the daily SLP fields. This will remove the impact of any far-field influence, for instance long-term trends (climate drift) or interannual variability (like the Southern Annular Mode).

For days with weak net winds (CE), the polynya is usually sandwiched between the westerlies to the north and easterlies to the south. The response patterns are mostly localized and limited to the polynya region, consistent with the large temperature difference over the polynya between the surface (mostly open water close to the freezing point) and the overlying atmosphere (TS-TBOT). Sensible and latent heat fluxes (S+L HFLX), as well as 10 meter wind speed (U10) are significantly enhanced when a polynya is present. We can also see a small but significant increase in precipitation, while there is no noticeable impact on SLP and hence on the large-scale circulation.

For northeasterly winds (> 5 m s^{-1}; NE), the situation is more complex. These days are often associated with the arrival of a low-pressure system from the west. Again, a large temperature difference leads to locally enhanced fluxes of sensible and latent heat (S+L HFLX). We also observe a large signature in near-surface humidity, precipitation, and wind speed, in particular in the region downwind from the polynya. In addition, there is a significant large-scale anomaly in sea level pressure, with elevated high pressure northwest of the polynya, and anomalously low pressure west of it.

An illustrative case is shown in Fig. 5, which shows the evolution of the variables leading up to and following September 19 of polynya year 76 (analysis day 142), a day with northeasterly winds over the polynya. Day 141 shows relatively quiet (CE) conditions over the polynya, with low wind speeds (U10), large air-sea temperature contrast (TS-TBOT), and large sensible and latent heat fluxes (S+L HFLX). The polynya is in the dry and cold continental air regime (low QBOT). On day 142, a low-pressure system arrives from the west, covering the polynya in moist and relatively warm maritime air (high QBOT). Despite the reduced air/sea temperature contrast, turbulent heat fluxes are still strong due to the higher wind speeds associated with the front. The depression accelerates the easterlies between the polynya and the continent (vectors in PSL panel) and draws cold and dry continental air northward, resulting in relatively large ice-air temperature contrasts in the continental air zone just north of the continent. This air collides with the northeasterly flow of warm and moist maritime air, which gained moisture over the polynya. We surmise that this maritime air is forced upward, resulting in the band of strong precipitation southwest of the polynya. The following day, the depression has moved eastward, and so has the intensification of the easterlies. Precipitation has all but ceased. Although northeasterly wind events occur in both polynya and non-polynya years, the atmospheric modification taking place over the polynyas apparently has a significant impact on the precipitation, intensification of the easterlies, and deepening of the atmospheric surface pressure just west of the polynya.

For the northwesterly (NW), southwesterly (SW) and southeasterly (SE) wind directions (Fig. 4), the localized anomalies in sensible and latent heat fluxes, associated with the enhanced surface/air temperature contrast over polynyas, are clearly discernible. However, they are strongest for the southerly wind directions, when cold and dry continental air is advected northward over the polynya. We also see significantly enhanced humidity (QBOT) over the polynya, and in downstream plumes over the adjoining ice pack; enhanced wind speeds (U10); and enhanced precipitation, mostly on the downwind side of the polynya. For these three wind directions, surface pressure (SLP) shows a distinct minimum over the polynya. The difference in SLP between polynya and non-polynya years is not significant for NW; slightly significant for SW; and quite pronounced for SE. This suggests that polynyas indeed exert an impact on the overlying atmosphere and the regional circulation.

4. Summary, Discussion and Conclusion

In this note we studied the response of the atmosphere to polynyas in the ice pack of the Weddell Sea. We analyzed 6 years of a high-resolution coupled climate simulation, three years of which featured a polynya. Although the relatively small sample size makes it difficult to make conclusive statements, several features emerged robustly from the analysis of this specific simulation:

- Sensible and latent heat fluxes are significantly enhanced over the Weddell Polynya: total turbulent heat flux values are on average about 170 W m^{-2} higher, but values exceed 200 W m^{-2} for southerly wind conditions. These values are in good agreement with estimates of Moore et al. (2002), who found sensible and latent heat fluxes of the order of 150 W m^{-2} and 50 W m^{-2}, respectively;

- The Weddell Polynya has a significant impact on the structure of the clouds, as the polynya is associated with a higher deck of convective clouds with high water and ice content. Clouds in non-polynya years, on the other hand, are lower to the ground as well as optically much thinner, and probably reflect ice fog (Girard and Blanchet 2001). This distinction is in agreement with the study of Fitzpatrick and Warren (2007), who compared the optical properties of clouds over sea ice and open water. In contrast to Moore et al. (2002), we did not find a significant difference in overall cloud cover. We will discuss this in a bit more detail later on.

- Shortwave flux absorption is enhanced by about 100 W m^{-2}, due to the fact that the polynya's open water with a low albedo absorbs more solar radiation than sea ice, which has typical albedos varying between 0.3 and 0.5 for first-year ice, and up to 0.9 for snow covered ice (Brandt et al. 2005). The fact that the shortwave anomaly at the surface is of the same magnitude as at the top of the atmosphere suggests that the more substantial cloud deck over polynyas does not have a significant impact on the short-wave radiation balance;

- Surprisingly, no impact on the *net* surface longwave balance was found; the enhanced emission of longwave radiation from the surface of the polynya is almost exactly counteracted by increased downwelling fluxes from clouds, which were shown to have much higher liquid and ice content than the ice fog that covers the sea ice during non-polynya years. This is in contrast to Moore et al. (2002), who find that the impact of the cloud response on the longwave radiative budget is secondary in the (coarse-resolution) NCEP reanalysis;

- Specific humidity is significantly enhanced over the polynya, and in downstream moisture plumes over the ice pack. Also precipitation is enhanced by about 1 mm day^{-1}, in agreement with Moore et al. (2002). This enhancement takes place mostly on the downwind side, where indeed uplift is expected (Dare and Atkinson 1999);

- We found some support for the hypothesis that the polynya generates a thermal low pressure system, as predicted by Timmermann et al. (1999). However, this response was found to be statistically significant only for southerly wind directions that advect cold and dry continental air over the polynya. Moore et al. (2002) find 6-8 mbar lower sea level pressure over the Weddell Polynya compared to climatology, while Glowienka-Hense (1995) find values between 3 and 4 mbar; our values for southerly winds are more in line with the latter.

We found that the simulated cloud cover is very high (up to 95%) for both polynya and non-polynya years. For polynya years, such high cloud fractions seem to be consistent with observations. Carsey (1980), for instance, notes high cloudiness over the Weddell Polynya ("100% on most days"), and comparable values are characteristic of open-ocean conditions north of the seasonal ice zone (Bromwich et al. 2012). However, the model appears to overestimate cloud fraction during the non-polynya years. The compilation of (post Weddell Polynya) cloud observations by Bromwich et al. (2012) shows average winter and spring cloud fractions in the region between

65 and 80%. This is in agreement with Guest (1998), who observed overcast conditions 77% of the time over the ice pack in August 1994. The reanalysis of Moore et al. (2002) agrees that non-polynya conditions have about 20% less cloud cover than polynya conditions.

We found that the northeasterly wind direction generates the strongest response of the atmosphere, with -on average- a significant strengthening of the easterlies adjacent to the continent, and a downstream plume of precipitation that is apparently generated by the uplift of the warm and moisture-laden polynya air when it collides with the contintal winds. The response of the atmospheric pressure pattern shows a significant lowering of the PSL downstream of the polynya. This pattern is robustly reproduced, even after subsampling the NE days every third day. The dynamics of this response is not clear and will require further analysis.

This study confirms that large open-ocean polynyas have a significant local impact on the overlying atmosphere. Regional-scale impacts are also clear from the current analysis, but depend strongly on the synoptic wind direction. Most notably this study reveals the usefulness of analyzing the output of state-of-the-art high-resolution ESMs to enhance our understanding of intricate coupled phenomena that may simply not emerge in coarse-resolution ESM simulations. Here, we first find that a Weddell Polynya emerges only in the high-resolution simulations, which in its own right is an issue to be investigated. Second, the high spatial resolution of the atmosphere component (CAM5) allows for detailed investigations of the polynya impact on the atmosphere in a complete coupled setting.

5. Citations

Acknowledgments. This research was supported by the Regional and Global Climate Modeling program of the US Department of Energy Office of Science, as contribution to the HiLAT project. Los Alamos National Laboratory is operated by the Los Alamos National Security, LLC for the National Nuclear Security Administration of the U.S. Department of Energy under contract DE-AC52-06NA25396. The authors thank Phil Rasch and Hailong Wang (PNNL) for useful comments. We thank J. Small (NCAR) and his colleagues for generously making this data available through the Earth System Grid (www.earthsystemgrid.org).

References

Adolphs, U., and G. Wendler, 1995: A pilot study on the interactions between katabatic winds and polynyas at the Adélie Coast, eastern Antarctica. *Antarctic Science*, **7**, 307–314.

Andreas, E. L., W. B. Tucker, and S. F. Ackley, 1984: Atmospheric boundary-layer modification, drag coefficient, and surface heat flux in the Antarctic marginal ice zone. *J. Geophys. Res.*, **89**, 649–661.

Arbetter, T. E., A. H. Lynch, and D. A. Bailey, 2004: Relationship between synoptic forcing and polynya formation in the Cosmonaut Sea: 1. Polynya climatology. *J. Geophys. Res.*, **109 (C4)**.

Bailey, D. A., A. H. Lynch, and T. E. Arbetter, 2004: Relationship between synoptic forcing and polynya formation in the Cosmonaut Sea: 2. Regional climate model simulations. *J. Geophys. Res.*, **109 (C4)**.

Brandt, R. E., S. G. Warren, A. P. Worby, and T. C. Grenfell, 2005: Surface albedo of the Antarctic sea ice zone. *J. Climate*, **18 (17)**, 3606–3622.

Bromwich, D. H., and Coauthors, 2012: Tropospheric clouds in Antarctica. *Rev. Geophys.*, **50 (1)**.

Carsey, F., 1980: Microwave observation of the Weddell Polynya. *Mon. Wea. Rev.*, **108 (12)**, 2032–2044.

Cheon, W. G., S.-K. Lee, A. L. Gordon, Y. Liu, C.-B. Cho, and J. J. Park, 2015: Replicating the 1970s' Weddell Polynya using a coupled ocean-sea ice model with reanalysis surface flux fields. *Geophys. Res. Lett.*, **42 (13)**, 5411–5418.

Comiso, J., and A. Gordon, 1987: Recurring polynyas over the Cosmonaut Sea and the Maud Rise. *J. Geophys. Res.*, **92 (C3)**, 2819–2834.

Comiso, J. C., and A. L. Gordon, 1996: Cosmonaut polynya in the Southern Ocean: Structure and variability. *J. Geophys. Res.*, **101 (C8)**, 18 297–18 313.

Dare, R., and B. Atkinson, 1999: Numerical modeling of atmospheric response to polynyas in the Southern Ocean sea ice zone. *J. Geophys. Res.*, **104 (D14)**, 16 691–16 708.

Dare, R., and B. Atkinson, 2000: Atmospheric response to spatial variations in concentration and size of polynyas in the Southern Ocean sea-ice zone. *Boundary-layer meteorology*, **94 (1)**, 65–88.

de Lavergne, C., J. B. Palter, E. D. Galbraith, R. Bernardello, and I. Marinov, 2014: Cessation of deep convection in the open Southern Ocean under anthropogenic climate change. *Nature Clim. Change*, **4 (4)**, 278–282.

Downes, S. M., and Coauthors, 2015: An assessment of Southern Ocean water masses and sea ice during 1988–2007 in a suite of interannual CORE-II simulations. *Ocean Model.*, **94**, 67–94.

Fitzpatrick, M. F., and S. G. Warren, 2007: The relative importance of clouds and sea ice for the solar energy budget of the Southern Ocean. *Journal of Climate*, **20 (6)**, 941–954.

Girard, E., and J.-P. Blanchet, 2001: Microphysical parameterization of Arctic diamond dust, ice fog, and thin stratus for climate models. *J. Atmos. Sci.*, **58 (10)**, 1181–1198.

Glowienka-Hense, R., 1995: GCM response to an Antarctic polynya. *Contributions to Atmospheric Physics*, **68**, 303–317.

Gordon, A. L., 1982: Weddell deep water variability. *J. Mar. Res.*, **40**, 199–217.

Gordon, A. L., M. Visbeck, and J. C. Comiso, 2007: A Possible Link between the Weddell Polynya and the Southern Annular Mode. *J. Climate*, **20 (11)**, 2558–2571.

Guest, P. S., 1998: Surface longwave radiation conditions in the eastern Weddell Sea during winter. *J. Geophys. Res.*, **103 (C13)**, 30 761–30 771.

Heuzé, C., K. J. Heywood, D. P. Stevens, and J. K. Ridley, 2013: Southern Ocean bottom water characteristics in CMIP5 models. *Geophys. Res. Lett.*, **40 (7)**, 1409–1414.

Holland, D., 2001: Explaining the Weddell Polynya–a large ocean eddy shed at Maud Rise. *Science*, **292 (5522)**, 1697–1700.

Hurrell, J. W., and Coauthors, 2013: The Community Earth System Model: a framework for collaborative research. *Bull. Amer. Meteor. Soc.*, **94**, 1339–1360.

Johnson, G. C., 2008: Quantifying Antarctic Bottom Water and North Atlantic Deep water volumes. *J. Geophys. Res.*, **113**, doi:10.1029/2007JC004477.

Maqueda, M., A. Willmott, and N. Biggs, 2004: Polynya dynamics: a review of observations and modeling. *Rev. Geophys.*, **42 (1)**.

Martinson, D. G., P. D. Killworth, and A. L. Gordon, 1981: A convective model for the Weddell Polynya. *J. Phys. Oceanogr.*, **11 (4)**, 466–488.

Minnett, P., and E. Key, 2007: Meteorology and atmosphere–surface coupling in and around polynyas. *Elsevier Oceanography Series*, **74**, 127–161.

Moore, G., K. Alverson, and I. Renfrew, 2002: A reconstruction of the air-sea interaction associated with the Weddell Polynya. *J. Phys. Oceanogr.*, **32 (6)**, 1685–1698.

Prasad, T., J. L. McClean, E. C. Hunke, A. J. Semtner, and D. Ivanova, 2005: A numerical study of the western Cosmonaut polynya in a coupled ocean–sea ice model. *J. Geophys. Res.*, **110 (C10)**.

Small, R. J., and Coauthors, 2014: A new synoptic scale resolving global climate simulation using the Community Earth System Model. *J. Adv. Model. Earth Sy.*, **6 (4)**, 1065–1094.

Smith, S. D., R. D. Muench, and C. H. Pease, 1990: Polynyas and leads: an overview of physical processes and environment. *J. Geophys. Res.*, **95 (C6)**, 9461–9479.

Smith Jr., W. O., and L. I. Gordon, 1997: Hyperproductivity of the Ross Sea (Antarctica) polynya during austral spring. *Geophys. Res. Lett.*, **24 (3)**, 233–236.

Stössel, A., D. Notz, F. A. Haumann, H. Haak, J. Jungclaus, and U. Mikolajewicz, 2015: Controlling high-latitude Southern Ocean convection in climate models. *Ocean Model.*, **86**, 58–75.

Stössel, A., K. Yang, and S.-J. Kim, 2002: On the role of sea ice and convection in a global ocean model. *J. Phys. Oceanogr.*, **32 (4)**, 1194–1208.

Timmermann, R., P. Lemke, and C. Kottmeier, 1999: Formation and maintenance of a polynya in the Weddell Sea. *J. Phys. Oceanogr.*, **29 (6)**, 1251–1264.

von Storch, H., and F. W. Zwiers, 1999: *Statistical analysis in climate research*. Cambridge University Press, Cambridge, United Kingdom, 484 pp. pp.

Williams, W., E. Carmack, and R. Ingram, 2007: Physical oceanography of polynyas. *Elsevier Oceanography Series*, **74**, 55–85.

Zwally, H. J., J. Comiso, and A. Gordon, 1985: Antarctic offshore leads and polynyas and oceanographic effects. *Oceanology of the Antarctic Continental Shelf*, 203–226.

Zwally, H. J., and P. Gloersen, 1977: Passive microwave images of the polar regions and research applications. *Polar Record*, **18 (116)**, 431–450.

LIST OF TABLES

Table 1. Total number of days (percentage in brackets) for each wind direction category, for the Aug-Sep-Oct trimester of the three polynya (left) and non-polynya (right) years. The total number of days in each column adds up to 276. 23

TABLE 1. Total number of days (percentage in brackets) for each wind direction category, for the Aug-Sep-Oct trimester of the three polynya (left) and non-polynya (right) years. The total number of days in each column adds up to 276.

	Number of days in polynya years	Number of days in non-polynya years
CE	75 (27%)	78 (28%)
NE	37 (13%)	36 (13%)
NW	53 (19%)	41 (15%)
SW	76 (28%)	82 (30%)
SE	35 (13%)	39 (14%)

LIST OF FIGURES

Fig. 1. Sea ice fraction for the 3 polynya years, averaged over the Aug-Sept-Oct trimester. Black contours indicate the 15% limits for the monthly averages, while the red contour indicates the ‘polynya mask’ for non-polynya years, based on the 45% contour of sea ice fraction averaged over the 3 polynya years. The ‘island’ in year 80 reflects an area of elevated (30%) sea ice fraction within the polynya during August of that year. 25

Fig. 2. Seasonal evolution of sea ice fraction (ICEFRAC) and different atmospheric variables for the three polynya years (thin red), the three non-polynya years (thin blue), and their averages (thick lines). Shown are monthly-averaged values. Variables shown are surface temperature (TS), atmospheric temperature (TBOT) and humidity (QBOT) at the near-surface, wind speed at 10 m (U10), sensible (SHFLX) and latent (LHFLX) heat flux, net shortwave balance at the top of the atmosphere (FSNT), net longwave balance at the surface (FLNS), total cloud fraction (CLDTOT), precipitation rate (PRECT), and atmospheric surface pressure (PSL). 26

Fig. 3. Vertical profiles of ASO-averaged quantities, horizontally averaged over the polynya areas, for the three polynya years (thin red), the three non-polynya years (thin blue), their averages (thick lines), and their difference (black). Variables shown are cloud fraction (CLOUD), relative humidity (RELHUM), specific humidity (Q), in-cloud liquid (ICLDLWP) and ice (ICLDIWP) water path, temperature (T), vertical heat advection (-OMEGAT), and turbulent kinetic energy (TKE). 27

Fig. 4. Differences of atmospheric variables between polynya and non-polynya years, separated according to daily wind direction. ‘CE’ indicate averages over days with polynya-averaged wind-speed smaller than 5 m s^{-1}, regardless of direction. Other categories indicate averages over days with wind speeds exceeding 5 m s^{-1} and coming from the direction indicated. Yellow stippling indicates regions where the polynya and non-polynya means are significantly different at 95%, according to a t-test. Arrows in the ‘U10’ plot indicate wind pattern averaged over the polynya years. Red contour indicates 45% contour of sea ice fraction averaged over polynya years (ASO only). Variables shown are the sum of sensible and latent heat fluxes (S+L HFLX); temperature difference between surface and atmosphere (TS-TBOT); humidity in the near-surface layer (QBOT); precipitation (PRECT); wind speed at 10 m (U10); and sea level pressure (PSL). 28

Fig. 5. Evolution of select variables for September 18-20 of polynya year 76. 29

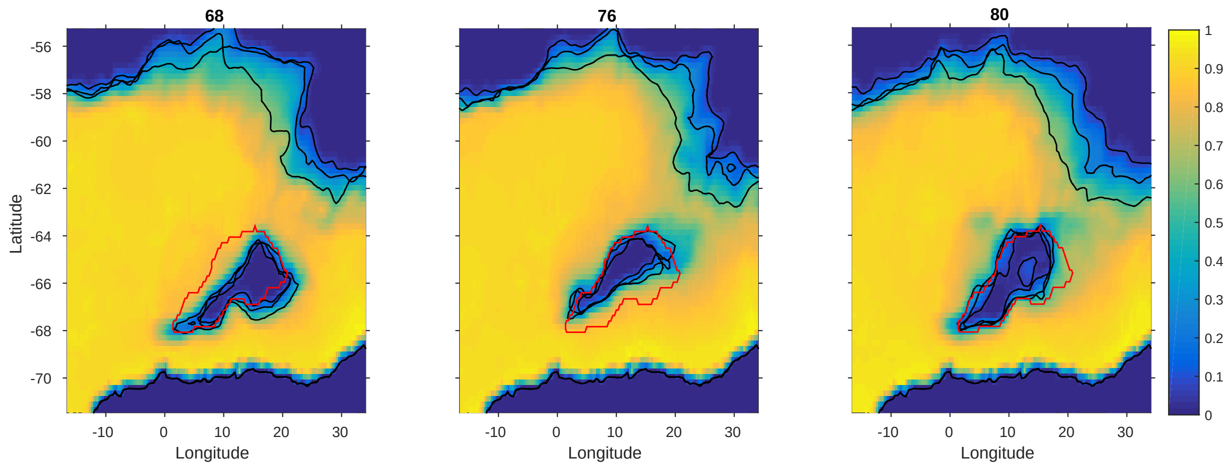

FIG. 1. Sea ice fraction for the 3 polynya years, averaged over the Aug-Sept-Oct trimester. Black contours indicate the 15% limits for the monthly averages, while the red contour indicates the 'polynya mask' for non-polynya years, based on the 45% contour of sea ice fraction averaged over the 3 polynya years. The 'island' in year 80 reflects an area of elevated (30%) sea ice fraction within the polynya during August of that year.

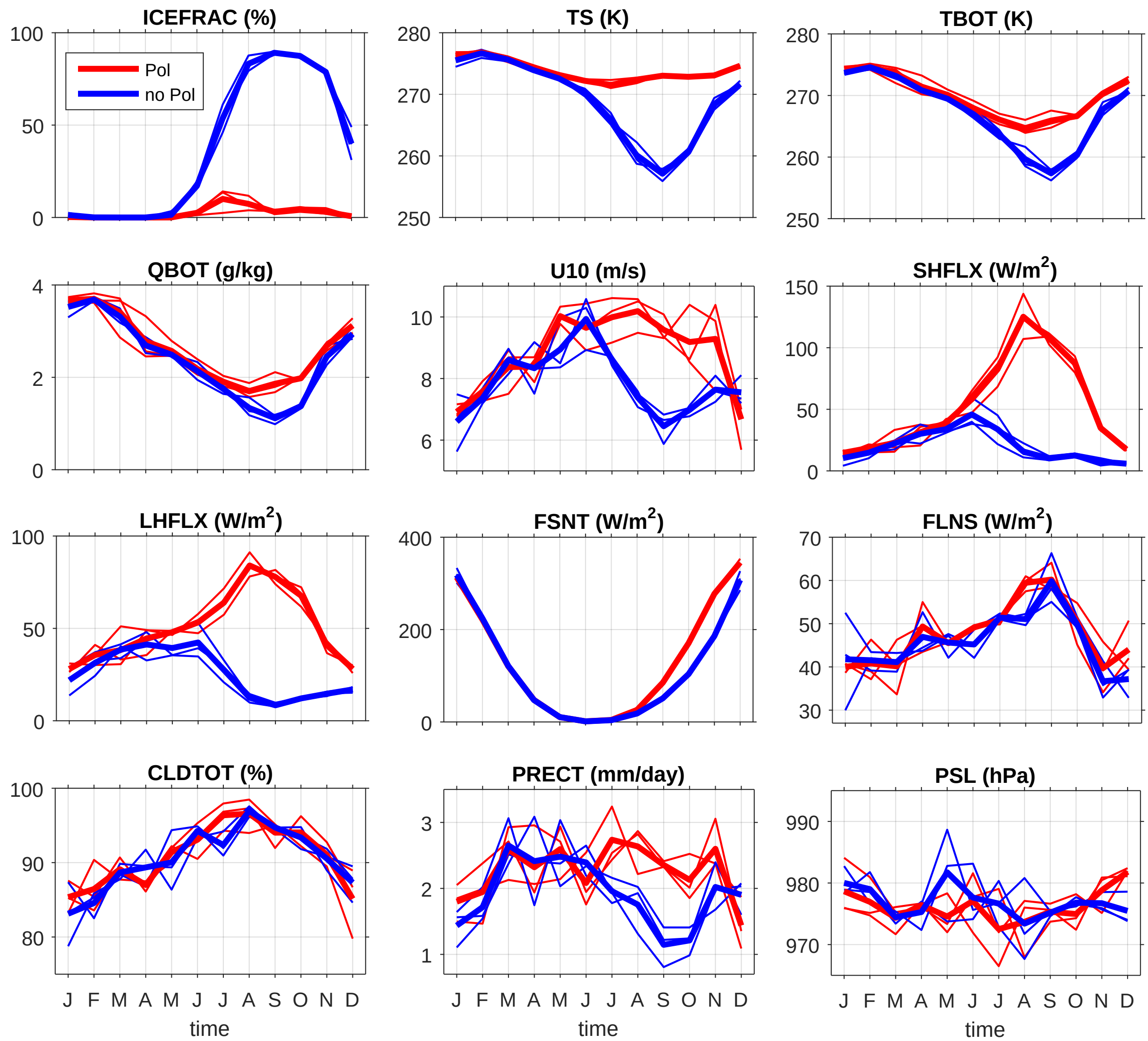

FIG. 2. Seasonal evolution of sea ice fraction (ICEFRAC) and different atmospheric variables for the three polynya years (thin red), the three non-polynya years (thin blue), and their averages (thick lines). Shown are monthly-averaged values. Variables shown are surface temperature (TS), atmospheric temperature (TBOT) and humidity (QBOT) at the near-surface, wind speed at 10 m (U10), sensible (SHFLX) and latent (LHFLX) heat flux, net shortwave balance at the top of the atmosphere (FSNT), net longwave balance at the surface (FLNS), total cloud fraction (CLDTOT), precipitation rate (PRECT), and atmospheric surface pressure (PSL).

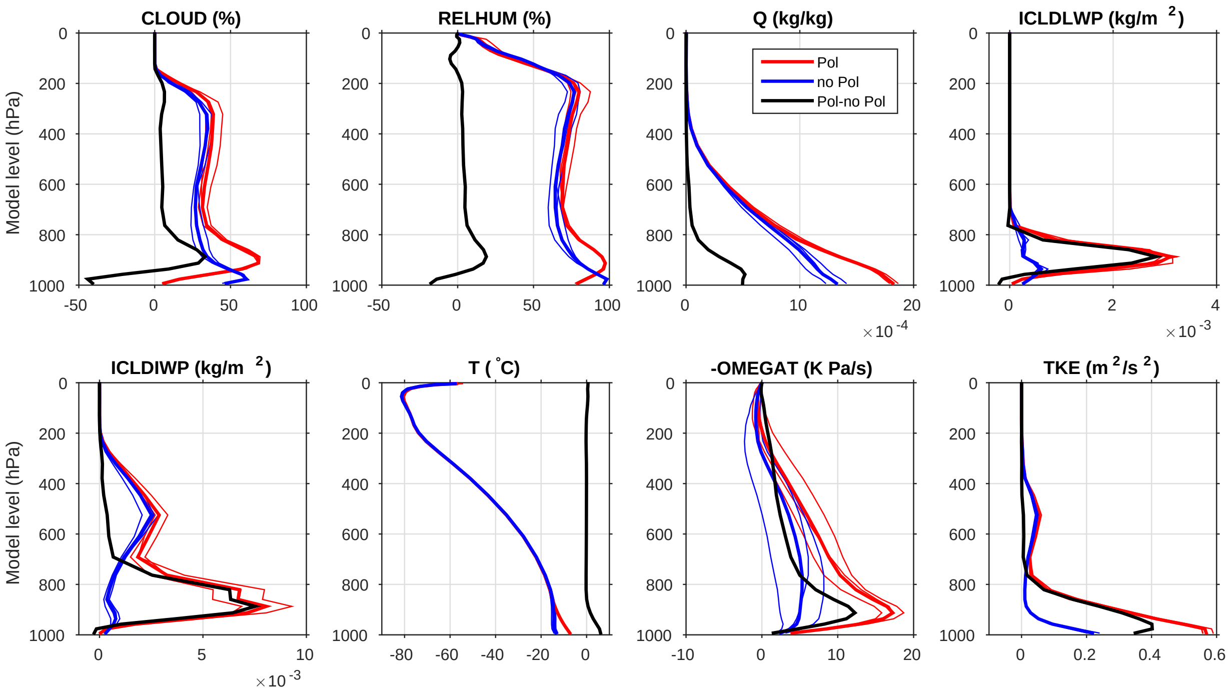

FIG. 3. Vertical profiles of ASO-averaged quantities, horizontally averaged over the polynya areas, for the three polynya years (thin red), the three non-polynya years (thin blue), their averages (thick lines), and their difference (black). Variables shown are cloud fraction (CLOUD), relative humidity (RELHUM), specific humidity (Q), in-cloud liquid (ICLDLWP) and ice (ICLDIWP) water path, temperature (T), vertical heat advection (-OMEGAT), and turbulent kinetic energy (TKE).

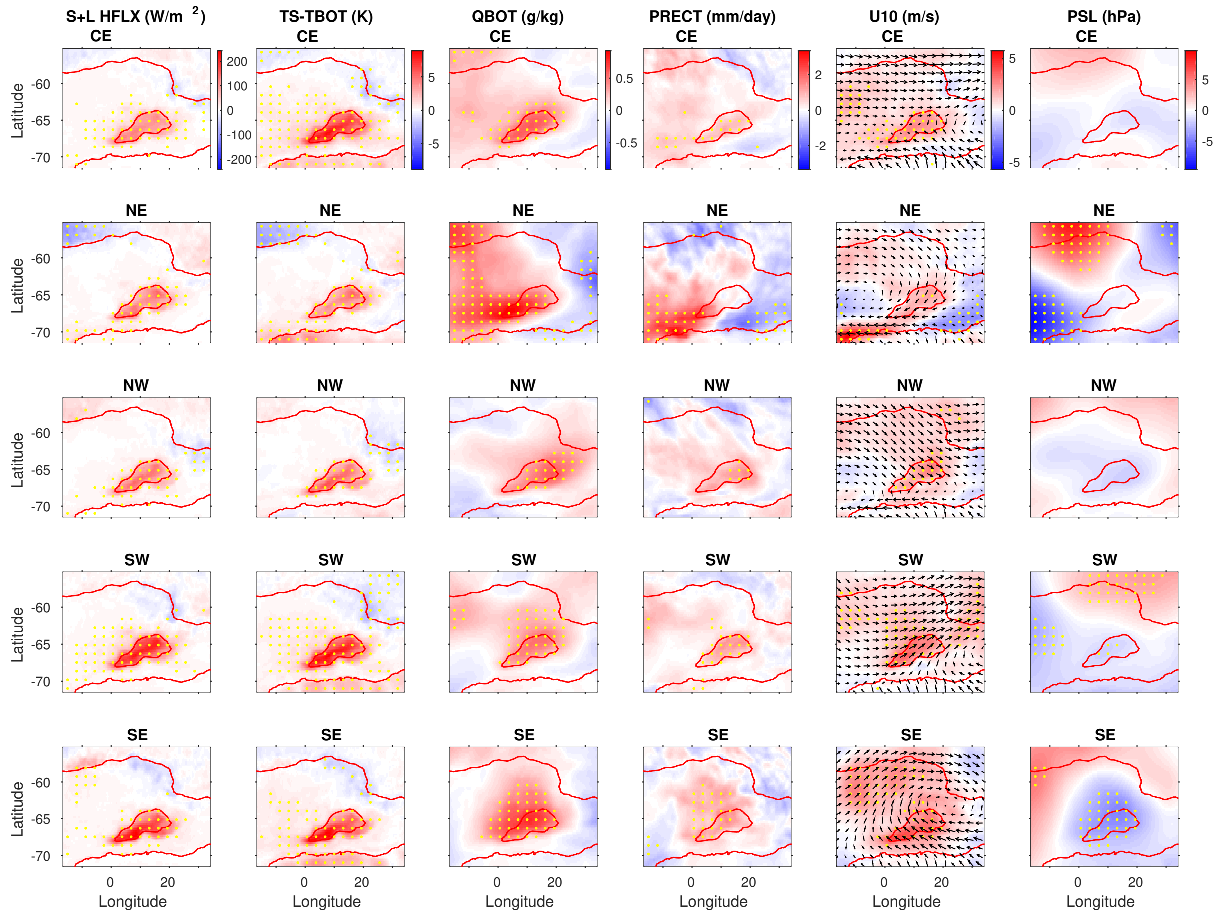

FIG. 4. Differences of atmospheric variables between polynya and non-polynya years, separated according to daily wind direction. 'CE' indicate averages over days with polynya-averaged wind-speed smaller than 5 m s^{-1}, regardless of direction. Other categories indicate averages over days with wind speeds exceeding 5 m s^{-1} and coming from the direction indicated. Yellow stippling indicates regions where the polynya and non-polynya means are significantly different at 95%, according to a t-test. Arrows in the 'U10' plot indicate wind pattern averaged over the polynya years. Red contour indicates 45% contour of sea ice fraction averaged over polynya years (ASO only). Variables shown are the sum of sensible and latent heat fluxes (S+L HFLX); temperature difference between surface and atmosphere (TS-TBOT); humidity in the near-surface layer (QBOT); precipitation (PRECT); wind speed at 10 m (U10); and sea level pressure (PSL).

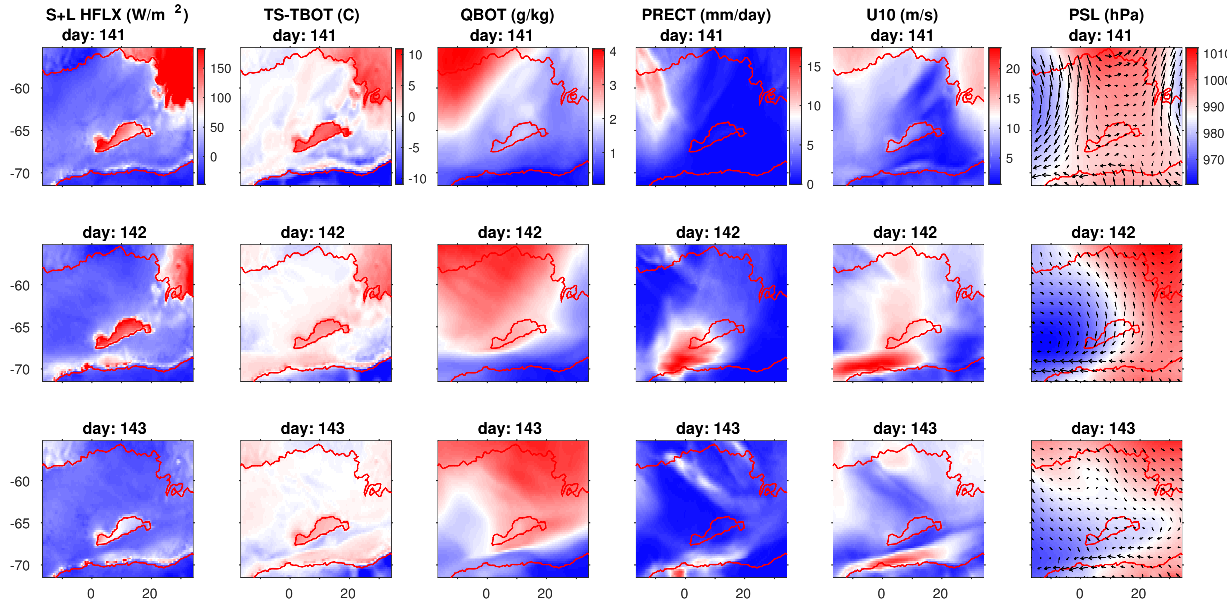

FIG. 5. Evolution of select variables for September 18-20 of polynya year 76.